Available online at www.elixirpublishers.com (Elixir International Journal)

Corrosion and Dye

Elixir Corrosion & Dye 87 (2015) 35491-35500

ISSN: 2229-712X

Thiazolidine Derivatives as Corrosion Inhibitors for Copper in Nitric Acid Solutions

A.S. Fouda[1,*], G. Elewady[1], A.A. Hassan[2] and R. Rady[1]

[1]Chemistry Department, Faculty of Science, Mansoura University, Mansoura-35516, Egypt.

[2]Chemistry Department, Faculty of Science, Damanhur University, Damanhur, Egypt.

ARTICLE INFO

Article history:

Received: 3 May 2011;

Received in revised form:

23 September 2015;

Accepted: 29 September 2015;

Keywords

Corrosion inhibition,

Copper,

HNO_3,

Thiazolidine derivatives.

ABSTRACT

Inhibition of copper corrosion by some thiazolidine derivatives in 1 M HNO_3 was inspected by" WL (weight loss), (EIS) electrochemical impedance spectroscopy, (EFM) electrochemical frequency modulation and potentiodynamic polarization measurements". The inhibition effectiveness increase by the increasing the concentration of inhibitor and deceased when temperature increased. It is clearly that these compounds work as mixed type inhibitors and that was proven by potentiodynamic polarization study. These inhibitors whose adsorption was found to obey Langmuir adsorption isotherm. Relationships of quantum structure-movement have been utilized to examine the molecular structure of the inhibitors efficiency. The surface morphology of copper specimen was analyzed by scanning electron microscopy (SEM).

Introduction

Copper is utilized broadly as a part of industry, as a result of his warm conductivity and mechanical properties. Copper is a moderately noble metal [1-5]. Nevertheless, it responds effortlessly in conventional situations containing oxygen. Thus, the investigation of its corrosion inhibition has reported in much consideration. Copper corrosion depends on the way of nature as well as of the state of utilization on materials. The most used methods for copper corrosion protection is the utilization of organic inhibitors. The majority of the understood acid inhibitors are organic compounds containing O, S, P and /or N atoms [6-9] these atoms enhance the activity of corrosion inhibitor. The corrosion inhibition of organic compounds is identified with their adsorption properties. Adsorption relies on upon the nature and the condition of the metal surface, on the kind of corrosive medium and on the chemical structure of the inhibitor [10]. Studies report that the adsorption of the organic inhibitors for the most metals and alloys on upon some Physico-chemical properties of the particle identified with its utilitarian group, steric effects, electronic density of giver atoms; Also, the presence of π-orbitals of the inhibitor with d-orbitals of the surface atoms, which actuate more prominent adsorption of the inhibitor particles onto the surface of copper, leading to the arrangement of corrosion formed film [11, 12]. The chemical active molecules of some of these inhibitors like azoles [13-15], amines and amino acids [16-18] among others performed better in copper. 1,2,3-Benzotriazole (BTAH, $C_6H_5N_3$) has also been tested to be effective corrosion inhibitor for copper and its amalgams. Mountassir and Srhiri [19] used AMT as corrosion inhibitor in sodium chloride medium. Deslouis *et al.* [15] studied the behaviour of copper in neutral aerated solution with some derivatives. Quantum chemical calculations have been broadly used to estimate the reaction mechanism [20].

The present work was intended to think about the corrosion inhibition of copper in 1M HNO_3 solutions by some thiazolidine derivatives as corrosion inhibitors utilizing chemical and electrochemical procedures, also to compare the experimental results with the theoretical ones.

Experimental methods

Solutions and materials

Copper specimens (99.98%) were utilized in the performance of experiments. Dilution of analytical reagent grade 70 % HNO_3 with bidistilled water which was used in the preparation of the corrosive solution and the various concentrations of thiazolidine derivatives for all studies. In this study, the thiazolidine derivatives presented in Table 1, which is tested as corrosion inhibitor was synthesized according to our used and known experimental methods [21]. The concentrations of inhibitors employed were varied from 1x 10^{-6} M to 21 x 10^{-6} M. A freshly prepared solution was utilized for each experiment.

WL tests

Seven parallel copper sheets of 2x2x2 cm were abraded with different grades of emery paper up to 1200 grit and after that washed with bidistilled water and acetone. In the experiments the copper sheets were dipped in 100 ml HNO_3 solution with and without various concentrations of inhibitors. After 3 hrs, the samples were taken out, washed, dried, and measured precisely. (IE) the inhibition efficiency and (θ) the degree of surface coverage of the inhibitors that were used on the corrosion of copper and were obtained as follows [22]:

"%IE=θx100=[1-(W/W°)]×100" (1)

Where W and W° and W are the average data of weight losses with and without addition of the inhibitor, respectively

Electrochemical measurements

"Potentiodynamic polarization measurements"

Electrochemical measurements were performed utilizing an ordinary three-compartment glass cell comprising of the copper example as working electrode (1cm^2), saturated calomel electrode (SCE) as reference electrode, and a platinum sheet (1cm^2) as a counter electrode. A Luggin capillary was joined to the reference electrode and to minimize IR drop the tip of the Luggin tube is made near to the surface of the working electrode. Under unstirred conditions estimations were done in solutions open to environment. All potentials were recorded versus SCE.

Tele: +2 050 2365730

E-mail addresses: asfouda@hotmail.

The electrode was treated as before, degreased with acetone, also washed with bidistilled water, and dried before each experiment. Curves of Tafel were gotten by changing the electrode potential. Stern-Geary method, utilized for the determination of corrosion current is performed by extrapolation of anodic and cathodic Tafel lines to a point which gives (log i_{corr}) and the corresponding corrosion potential (E_{corr}) for inhibitor free acid and for each concentration of inhibitor. Then (i_{corr}) was utilized for calculation of inhibition efficiency (%IE) and (θ) surface coverage as in equation 2:

$$\%IE = \theta \times 100 = [1- (i_{corr(inh)}/i_{corr(free)})] \times 100 \quad (2)$$

where $i_{corr(free)}$ and $i_{corr(inh)}$ are the corrosion current densities in the absence and presence of inhibitor, respectively .

(EIS) method

Measurements of impedance were completed in frequency range (0.1Hz to 100 kHz) with adequacy of 5 mV peak-to-peak utilizing ac signals at open circuit potential. The parameter obtained from the examination of Nyquist are the R_{ct} resistance of charge transfer (diameter of high-frequency circle) and the C_{dl} double layer capacity. The efficiencies of inhibition and the surface coverage (θ) acquired from the impedance calculations were computed from comparison 3:

$$\%IE = \theta \times 100 = [1-(R^{\circ}_{ct}/R_{ct})] \times 100 \quad (3)$$

where "R^{o}_{ct} and R_{ct} are the charge transfer resistance in the absence and presence of inhibitor", respectively.

(EFM) method

By utilizing two frequencies 2 and 5 Hz, EFM was done. The base frequency was 0.1 Hz, so the waveform reached after 1 s. The higher frequency should likewise be adequately moderate that the charging of the twofold layer does not add to the present reaction. Often, 10 Hz is a sensible limit. The Intermodulation spectra contain current reactions alloted for intermodulation and harmonical current tops[23-25] The vast crests were utilized to ascertain the corrosion current density (i_{corr}), the Tafel slopes (β_a and β_c) and the causality factors CF-2& CF-3[26]. The electrode potential was permitted to balance out 30 min before beginning the estimations. Every one of the trials were directed at 25°C.

Quantum chemical calculations

The molecular structures of the examined compounds were enhanced at first with PM3 semi empirical method in order to accelerate the figurings. All the quantum chemical calculations were performed with Material studio V. 6.0.

(SEM) method

The surface of copper was examined by scanning electron microscope (JEOL JSM-5500) previously, then after the fact submersion in 1 M HNO_3 test solution in the absence and in presence of the concentrations of the inhibitors at 25°C, for two days immersion. The samples were washed with bidistilled water, then dried and analyzed with no further treatments.

Results and Discussion

Chemical method (WL method)

WL of copper was resolved, at different time interims, in the nonattendance and vicinity of distinctive concentrations of compound (1). The acquired WL time bends are represented in Figure 1 for compound (1), the best one. Similar bends were gotten for other inhibitor (not indicated). The inhibition effectiveness of inhibitors was discovered to be subject to the inhibitor fixation. The bends acquired in the vicinity of inhibitors fall essentially underneath that of free acid. In all cases, the increment in the inhibitor fixation was joined by a reducing in weight-loss and an increment in the inhibition rate. These outcomes lead to the conclusion that these mixes are genuinely productive as inhibitors for copper dissolution in nitric acid solution. Also, the level of surface scope (Θ) was calculated from Eq.(1), would increment by expanding the inhibitor conc. Keeping in mind the end goal to get a near view, the variety of the rate inhibition (% IE) of the two inhibitors with their molar concentrations was computed by Eq. (1). The qualities acquired are condensed in Table 2. Cautious investigation of these outcomes demonstrated that, at the same inhibitor concentration, the request of inhibition proficiency is as follows: 1 > 2

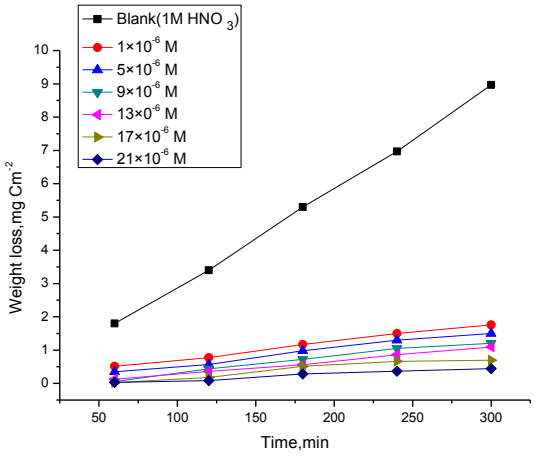

Figure 1. WL-time curves for the corrosion of copper in 1 M HNO_3 in the presence and absence of various concentrations of inhibitor (1) at 25 °C

Effect of temperature

The effect of heat on the corrosion rate of copper in 1M HNO_3 and in vicinity of various inhibitors was considered in the temperature range of 298–318K utilizing weight loss tests. Comparable curves were gotten for different inhibitors (not shown). As the heat increases, the rate of corrosion increases and the inhibition effectiveness of the added substances decreases as indicated in Table 3 for inhibitor (1) the best one. The adsorption of inhibitors on copper surface happens through physical adsorption.

Adsorption isotherms

To fit θ qualities, different adsorption isotherms were used, but by applying Langmuir adsorption isotherm, the results were found the best fit which is represented in Figure 2 for investigated inhibitors, Langmuir adsorption isotherm communicated by:

$$C/\theta = 1/K_{ads} + C \quad (4)$$

where C is the centralization (mol L^{-1}) of the inhibitor in the mass electrolyte, θ is the degree of surface scope (Θ = IE/100), K_{ads} is the adsorption equilibrium constant. A plot of C versus C/Θ should give straight line. In request to get a relative view, the variety of the adsorption equilibrium constant (K_{ads}) of the inhibitors with their molar concentrations was figured by equation (2). The results give great curves fitting for the connected adsorption isotherm as the relationship (R^2) coefficients were in the reach (0.943- 0.999). The data obtained are given in Table 4. These results confirm that these inhibitors are adsorbed on the metal surface through the protonated (N, S) atoms or by means of solitary pair of electrons of (N, S) atoms. The degree of inhibition is identified with the presence of adsorption layer of the inhibitors on metal surface. The equilibrium constant of adsorption K_{ads} got from the intercepts of Langmuir adsorption isotherm is identified with the free vitality of adsorption ΔG°_{ads} as follows:

$$K_{ads} = 1/55.5 \exp [^{-\Delta G^{\circ}ads]/RT} \quad (5)$$

where, 55.5 is the molar concentration of water in the solution in M^{-1}

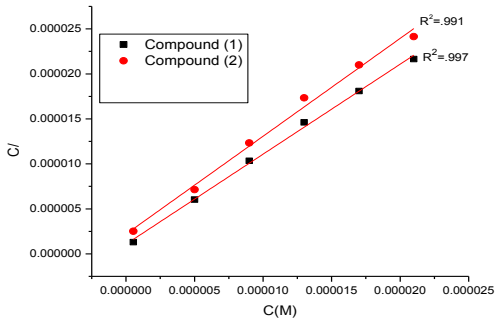

Figure 2. Langmuir adsorption isotherm of inhibitors on copper surface in 1 M HNO_3 at 25 °C

(ΔG^o_{ads}) against T Figure 3 gave the standard enthalpy of adsorption (ΔH^o_{ads}) and the standard entropy (ΔS^o_{ads}) as indicated by the thermodynamic fundamental mathematical statement 3:

$$\Delta G^o_{ads} = \Delta H^o_{ads} - T\Delta S^o_{ads} \quad (6)$$

Table 5 obviously demonstrates a decent relation between ΔG^o_{ads} and T, among thermodynamic parameters giving the great connection. The adsorption of studied inhibitors on copper surface from 1 M HNO_3 solution is spontaneous process and depends on the adsorbed layer on the copper surface. The negative sign of ΔG^o_{ads} reflects that the adsorption process is spontaneous. Generally, data of ΔG^o_{ads} around -20 kJ mol^{-1} or lower are reliable with the electrostatic attraction between the charged molecules and the charged metal (physical adsorption); those around -40 kJ mol^{-1} or higher involves charge sharing or exchange from organic molecules to the metal surface to frame a coordinate sort of bond (chemisorption) [27]. From the results of $\Delta G°_{ads}$ it was discovered the presence of far reaching chemical and physical adsorption). The unshared electron pairs in S, N may connect with d-orbitals of copper to give a defensive physical adsorbed film [28]. The estimations of thermodynamic parameter for the adsorption of inhibitors Table 5 can give important data about the system of corrosion inhibition. While an endothermic adsorption procedure (ΔH^o_{ads}> 0) is ascribed unequivocally to chemisorption [29], an exothermic adsorption process (ΔH^o_{ads}<0) may include either physisorption or chemisorption or blend of both procedures. In the displayed case, the computed qualities of ΔH°_{ads} for the adsorption of inhibitors in 1 M HNO_3 demonstrating that this inhibitors may be physically adsorbed. The qualities of $\Delta S°_{ads}$ in the vicinity of inhibitors are vast and negative that is went with exothermic adsorption procedure. This demonstrates that an increase in ordering takes place from going from reactants to the metal-adsorbed reaction complex [30].

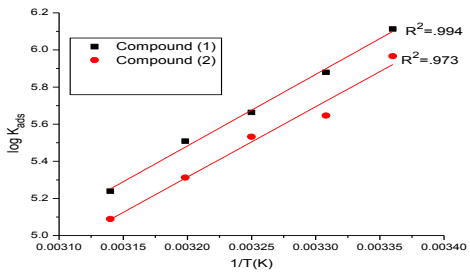

Figure 3. Variety of ΔG^o_{ads} against T for the adsorption of inhibitors on copper surface in 1M HNO_3 at various temperatures

Kinetic –thermodynamic corrosion parameters

The impact of heat on corrosion inhibition and corrosion of copper in 1 M HNO_3 solution in the deficiency and vicinity of diverse concentrations of investigated compounds at distinctive temperatures running from 25ºC to 45ºC was considered utilizing weight loss estimations. The corrosion rate increments with expanding temperature both in uninhibited and inhibited acid. The evident activation kinetic (E^*_a) for the corrosion procedure can be ascertained from Arrhenius-sort mathematical statement (12):

$$k_{cor\ r} = A \exp^{(E^*a/RT)} \quad (7)$$

where "E^*_a is the apparent kinetic of activation, R is the universal gas constant, T is the absolute temperature and A is the Arrhenius pre-exponential constant". Estimations of clear actuation vitality of corrosion for copper in 1 M HNO_3 (E^*_a = (incline) 2.303 x R) shown in Table 6, without and with different concentrations of compound (1) decided from the slant of log (k_{corr}) against1/T plots are demonstrated in Figure 4. Review of the information demonstrates that the enactment vitality is lower in the vicinity of inhibitors than in its deficiency. This was credited to moderate rate of inhibitor adsorption with a resultant closer way to deal with balance amid the analyses at higher temperatures according to Hoar and Holliday [31]. But, Riggs and Hurd [32] clarified that the diminishing in the initiation vitality of corrosion at larger amounts of inhibition emerges from a movement of the net corrosion reaction from the revealed piece of the metal surface to the secured one. Schmid and Huang [33] found that organic molecules inhibit both the anodic and cathodic incomplete responses on the terminal surface and a parallel response happens on the secured zone, be that as it may, the response rate on the secured territory is generously not exactly on the revealed range like the present study. The option definition of move state mathematical statement is indicated in Eq. (13):

$$k_{corr}=(RT/Nh)e^{(\Delta S^*/R)\exp(-\Delta H^*/RT)} \quad (8)$$

where $k_{corr}$is the rate of metal dissolution, h is Planck's constant, N is Avogadro's number, ΔS^* is the entropy of activation and ΔH^* is the enthalpy of activation.

Figure 5 shows a plot log (k_{corr}/T) against (1/T) on account of inhibitor (1) in 1 M HNO_3. Similar behavior is seen on account of inhibitor 2 (not shown). Straight lines are gotten with slants equivalent to (ΔH^*/2.303R) and intercepts are [log (R/Nh + ΔS^*/2.303R)] are calculated Table 6. The increase in E_a^* with increase inhibitor fixation Table 6 is commonplace of physical adsorption. The positive indications of the enthalpies (ΔH^*) mirror the endothermic way of the metal disintegration procedure. Data of entropies (ΔS^*) suggest that the enacted complex at the rate deciding step represents an affiliation as opposed to a separation step, implying that a decline in cluttering takes place on heading off from reactants to the enacted complex [34,35]. However, the quality of (ΔS^*) abatements bit by bit with expanding inhibitor concentrations in all the acid media.

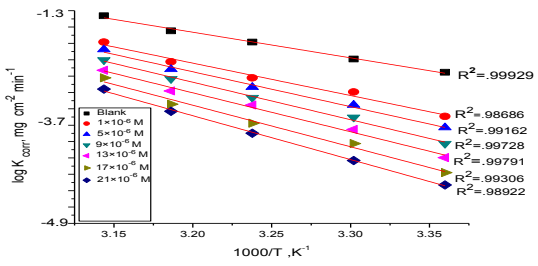

Figure 4. Arrhenius plots for copper corrosion rate (k_{corr}) (Log k against (1/T)) diagrams after 120 minute of dipping in 1M HNO_3 with and without of different concentrations of inhibitor (1)

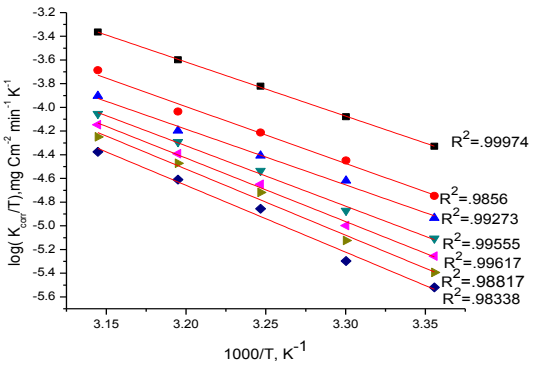

Figure 5. Transition plots for copper corrosion rates Log (k/T) against (1/T) curves after 120 minutes dipping in 1M HNO_3 with and without of different concentrations of inhibitor (1)

Potentiodynamic polarization measurements

Figure 6 shows the polarization curves of Cu in 1M HNO_3 for inhibitor 1 at 25ºC. The anodic polarization curve of copper in the inhibitor-free solution demonstrated a monotonic increase of current with potential until the current came to the greatest worth data. After this most extreme current density data, decreases current density quickly with increasing potential, In inhibitor vicinity, both the cathodic and anodic current densities were incredibly diminished over a wide potential territory. Different corrosion parameters for example corrosion potential (E_{corr}), anodic and cathodic Tafel slopes (β_a, β_c), the (i_{corr}) corrosion current density, the (θ) degree of surface coverage and the (%IE) inhibition efficiency are given in Table 7. It can resulted from the results of experiments, addition of inhibitors increase the cathodic and anodic currents. The data of E_{corr} were affected and changed slightly by the adding of inhibitors. This shows that these inhibitors go about as mixed-type inhibitors. Slopes of anodic and cathodic Tafel lines (β_a and β_c), were not changed (Tafel lines are parallel), in the increase of the concentrations of the tested compounds which shows that there is no change of the mechanism of inhibition with and without inhibitors. The inhibition effectiveness of all inhibitors at various concentrations as given by polarization tests are recorded in Table 7. The results are in great agreement with those got from WL measurements.

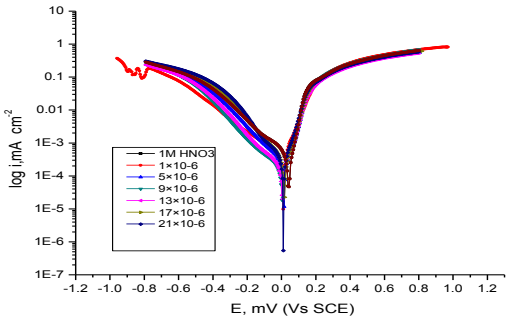

Figure 6. Polarization curves of copper in 1M HNO_3 with and without various concentrations of compound (1) at 25 ºC

(EIS methods)

EIS is nondestructive method and it is capable method for studying the corrosion. Surface characteristics, electrode kinetic and component data can be acquired from impedance graphs [36, 37]. Figure 7 demonstrates the Nyquist (a) and Bode (b) curves got at open-circuit potential without and with expanding concentrations of examined mixes at 25°C. The increment in the measure of the capacitive circle with the increasing of examined compounds demonstrates that an obstruction steadily shapes on the surface of Copper. (Figure 7a) An increase in the circle size capacitive improves, at an altered concentrations of inhibitor, their order as follow: (1) > (2), affirming the most noteworthy inhibitive impact of compound (1). (Figure 7b) Bode graphs, (log Z against. log f) demonstrates that the aggregate impedance increments with increasing inhibitor concentrations., and Bode graph (log f vs. phase) demonstrates an increase in the phase angle shift, relating with the increment in adsorption of inhibitor on the surface of copper. Ideal half circles of course from the hypothesis of EIS cannot be produced by the Nyquist graphs do not produce. The deviation from perfect half circle was for the most part l, credited to the scattering of frequency [38] and in addition to the surface inhomogenities.

The comparable circuit examined the EIS spectra of the explored mixes, Figure 8, that act as a solitary charge exchange reaction and work perfectly with the exploratory outcomes. CPE is presented in the circuit rather than twofold layer capacitor to give a more exact fit [39]. The twofold layer capacitance, C_{dl}, for a circuit including a CPE parameter (Y0 and n) were ascertained from mathematical statement 9 [40]:

$$C_{dl}=Y_0(\omega_{max})^{n-1} \quad (9)$$

whereY_0 is the magnitude of the CPE, the frequency at which the fanciful part of the impedance is maximal($\omega_{max} = 2\pi f_{max}$) and the variable n is a flexible parameter to examining the shape of the Nyquist graphs that for the most part lies between 0.5 and 1.0. Subsequent, it is clear that the graphs approaching by a solitary capacitive half circles, demonstrating that the corrosion procedure was the most part charged-exchange controlled [41, 42]. The public shape of the graphs is fundamentally the same for all examples (with and without inhibitors at various submersion times) demonstrating that no adjustment in the corrosion instrument [43]. From the impedance information Table 8, we conclude that the data of R_{ct} increments with expanding the fixation of the inhibitors and this demonstrate an increment in % IE_{EIS}, which in accord with the EFM outcomes acquired. The quality of R_{ct} in acidic solution can be improved by the vicinity of inhibitors. Data of twofold layer capacitance are likewise conveyed down to the most extreme degree in the vicinity of inhibitor and the reduction in the estimations of CPE follows the arrangement like that got for i_{corr} in this research. The lessening in CPE/C_{dl} results from a reduction in nearby dielectric steady and/or thickness increment in the of the twofold layer, suggesting that organic derivatives inhibit the copper corrosion by adsorption at metal/acid[44,45] .The inhibition proficiency was ascertained from the charge exchange resistance information from mathematical state[46] : where R^o_{ct} and Rct are the charge-transfer resistance data without and with inhibitor, respectively

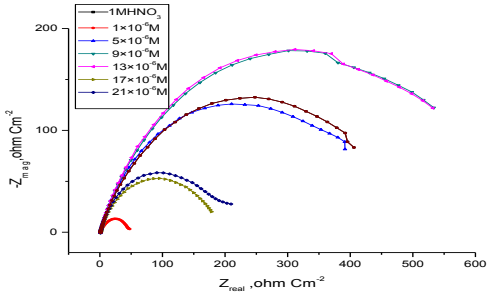

Figure 7a. Nyquist graphs for the copper corrosion in 1M HNO_3 without and with various concentrations of inhibitor (1) at 25ºC

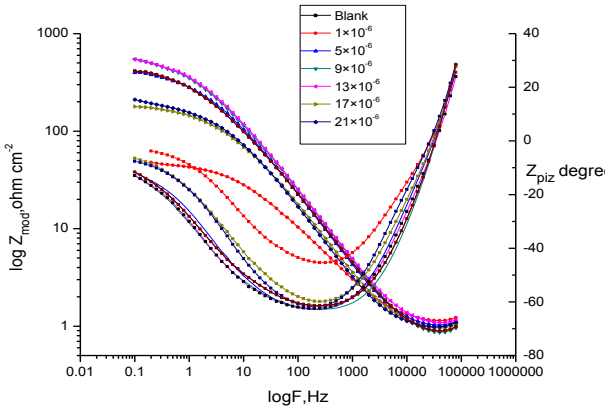

Figure 7b. The Bode graphs for the corrosion of copper in 1M HNO_3 without and with Various concentrations of inhibitor (1) at 25°C

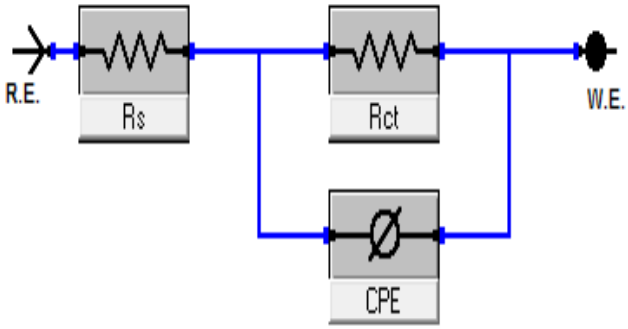

Figure 8. Experimental of EIS is improved by comparable circuit model

(EFM) methods

Nondestructive corrosion method used to estimate procedure that can specifically and rapidly concentrations the corrosion current data without earlier information of Tafel slopes, and with just a little polarizing signal. These preferences of EFM method make it an perfect possibility for online corrosion checking.47].The considerable strength of the EFM is CF which work as an inward keep an eye on the power of EFM estimations. CF-2 and CF-3 are figured from the frequency range of the present reactions.

Figure 9 demonstrates the EFM Intermodulation spectra" current vs frequency of copper in HNO_3 solution which contain various concentrations of compound (1). Curves for inhibitor 2 were obtained but not shown. The harmonic and intermodulation crests are very obvious and are much bigger than the foundation noise [48]. The increase in the concentration of compounds to the acidic solution diminishes the corrosion current density, showing that these mixes inhibit the corrosion of copper in 1 M HNO_3 from adsorption. CF acquired under various experimental conditions are more or less equivalent to the hypothetical qualities (2 and 3) demonstrating that the obtained information are checked and of great data. The inhibition efficiencies $\%IE_{EFM}$ increment by expanding the inhibitor concentrations and was figured as from mathematical statement. (10):

$$\%IE_{EFM} = [1-(i_{corr}/i^{o}_{corr})]\times 100 \quad (10)$$

where i^{o}_{corr} and i_{corr} are corrosion current densities in the without and with inhibitor, respectively. The inhibition adequacy acquired from this technique is in the order: (1) > (2)

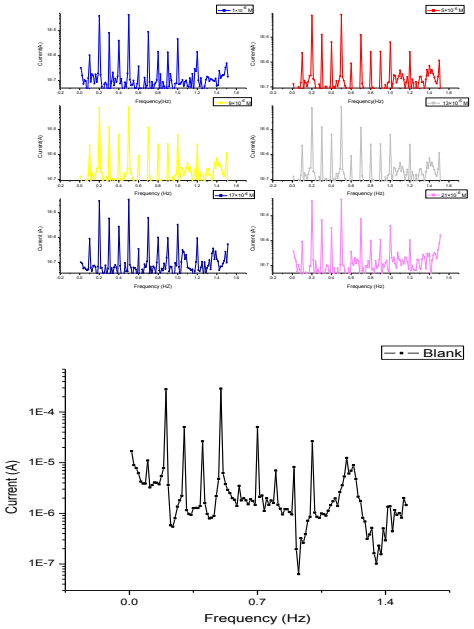

Figure 9. EFM spectra for copper in 1 M HNO_3 in the absence and presence of different concentrations of inhibitor (1) at 25°C

Surface morphology examination

To verify if the investigated compounds are really adsorbed on the surface of copper or just peeled off the surface, Scanning electron microscopy (SEM) and kinetic dispersive X-ray (EDX) experiments were carried out. SEM images were indicative of the changes that accompany both corrosion and protection of the copper surface Fig. 10(1-4). Figure 10 (1) shows the free metal. Figure 10(2) shows the damage caused to the surface by nitric acid. Figure 10(3, 4) shows SEM images of the copper surface after treatment with 1 M HNO_3 containing 21 x 10^{-6} M of investigated inhibitors. From these images, it is obvious that the copper surface seems to be almost unaffected by corrosion. This is because of adsorption of investigated inhibitors forming a thin protective film of the inhibitors on the metal surface. This film is responsible for the highly efficient inhibition by these inhibitors. The corresponding EDX profile analyses are presented in Table 10 and Figure 11 for investigated compounds. It is also important to notice the existence of C and N peaks in the EDX spectra of the copper surface corresponding to the samples immersed for 2 days in solutions containing the optimum concentration of these compounds. The formation of a thin inhibitor film is in agreement with the SEM observations.

Quantum chemical calculations

The E_{HOMO} demonstrates the capacity of the molecule to give electrons to specified acceptor with unfilled sub-atomic orbitals, while the E_{LUMO} shows its capacity to acknowledge electrons. The bring down the worth of E_{LUMO}, the more capacity of the molecule is to acknowledge electrons [49].

The most data of E_{HOMO} of the inhibitor, the less demanding is its capacity to offer electrons to the abandoned d-orbital of metal surface, and the more prominent is its inhibition ability. This is shown in Table 11, compound A has the highest data of E_{HOMO}, which indicate that this molecule has high capacities of charge donation to the metallic surface and has high inhibition efficiency.

Table 1. Chemical structures, names, molecular weights and molecular formulas of inhibitors

Inh.	Structures	Names	Mol. weights Mol Formulas
1	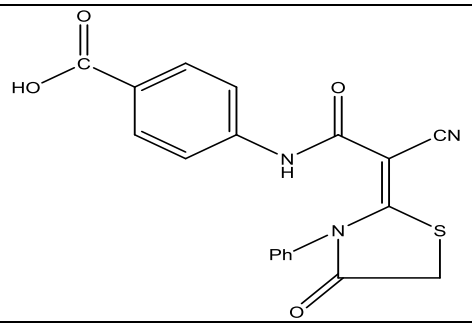	E)-4-(2-cyano-2-(4-oxo-3-phenylthiazolidin-2-ylidene) acetamido) benzoic acid	379 $C_{19}H_{13}O_4N_3S$
2	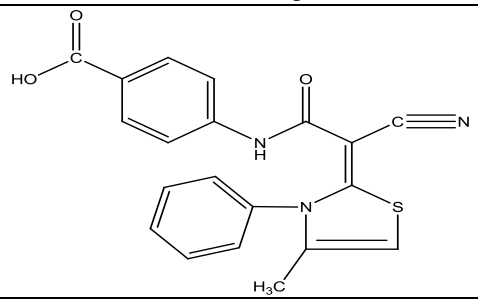	(E)-4-(2-cyano-2-(4-methyl-3-phenylthiazol-2(3H)-ylidene) acetamido) benzoic acid	377 $C_{20}H_{15}O_3N_3S$

Table 2. Variation of corrosion rate (CR) and inhibition productivity (% IE) of distinctive compounds with their molar concentrations at 25°C and at 120 min submersion in 1 M HNO_3.

"Compound	Conc. M	CR mg cm^{-2} min^{-1}	%IE
Blank	---	**0.0280**	----
1	$1X10^{-6}$	0.0066	76.4
	$5X10^{-6}$	0.0050	82.1
	$9X10^{-6}$	0.0036	87.1
	$13X10^{-6}$	0.0033	88.2
	$17X10^{-6}$	0.0017	93.9
	$21X10^{-6}$	0.0007	97.5
2	$1X10^{-6}$	0.0100	64.2
	$5X10^{-6}$	0.0092	67.1
	$9X10^{-6}$	0.0076	72.8
	$13X10^{-6}$	0.0075	73.2
	$17X10^{-6}$	0.0050	82.1
	$21X10^{-6}$	0.0039	86.1

Table 3. Estimations of corrosion rate (C.R) and of inhibition efficiencies %IE of inhibitor (1) to calculate the copper corrosion in 1 M HNO_3 from weight-loss estimations at distinctive Fixations at temperature range of 298-318 K

[inh] x 10^{-6}M	298K		303K		308K		313K		318K	
	C.R	% IE	C.R	%IE	C.R	%IE	C.R	%IE	C.R	%IE
Blank	0.0280	---	0.0350	---	0.0500	---	0.0750	---	0.1115	---
1	0.0066	76.4	0.0233	33.4	0.0337	32.6	.0512	31.7	0.0947	15.1
5	0.0050	82.1	0.0200	42.8	0.0290	41.9	0.0457	39.1	0.0900	19.2
9	0.0036	87.1	0.0154	55.9	0.0240	51.9	0.0400	46.6	0.0771	30.8
13	0.0033	88.2	0.0133	61.9	0.0235	52.9	0.0367	51.1	0.0666	40.2
17	0.0017	93.9	0.0100	71.4	0.0185	63.1	0.0317	57.7	0.0635	43.1
21	0. 0007	97.5	0.0088	74.8	0.0183	63.3	0.0310	58.7	0.0561	49.7

Table 4. Equilibrium constant (K_{ads}) of investigated compounds adsorbed on copper surface in 1M HNO_3 at 25°C

Temp °C	1		2	
	K_{ads} $x10^{-3}$ M^{-1}	R^2	K_{ads} $x10^{-3}$ M^{-1}	R^2
25	1296.6	0.995	925.5	0.985
30	313.1	0.987	280.8	0.979
35	460.3	0.985	340.5	0.972
40	428.7	0.979	205.3	0.969
45	173.4	0.976	122.8	0.965

Table 5. Thermodynamic parameters for the adsorption of inhibitors on Cu surface in 1M HNO_3 at different temperatures

Inhibitor	Temperature °C	$-\Delta G^o_{ads}$ kJ mol^{-1}	$-\Delta H^o_{ads}$ kJ mol^{-1}	$-\Delta S^o_{ads}$ J $mol^{-1}K^{-1}$
1	25	44.8	71.7	90.3
	30	42.1		98.1
	35	43.7		91.1
	40	44.2		87.9
	45	42.5		91.9
2	25	44.0	73.9	100.6
	30	41.7		106.4
	35	42.9		100.8
	40	42.3		101.2
	45	41.6		101.8

Table 6. Activation parameters for copper corrosion without and with different concentrations of inhibitors in 1M HNO_3

Inhibitor	[inh]$x10^{-6}$ M	E_a^* kJ mol^{-1}	ΔH^* kJ mol^{-1}	$-\Delta S^*$ J $mol^{-1}K^{-1}$
Blank	-------	60	28	105
1	1	76	40	82
	5	71	42	63
	9	74	50	53
	13	77	54	44
	17	78	58	33
	21	79	67	29
2	1	67	29	101
	5	68	31	90
	9	69	34	81
	13	70	39	62
	17	71	43	51
	21	72	50	44

Table 7. Tafel slopes (β_c, β_a), corrosion current density (i_{corr}), inhibition effectiveness (% IE) Corrosion potential (E_{corr}) and degree of surface coverage (θ) of copper in 1 M HNO_3 at 25°C" for investigated compounds.

Inh.	[inh] $x10^{-6}$M	$-E_{corr}$ mV vs SCE	$i_{corr}x10^{-4}$ µA cm^{-2}	β_a mV dec^{-1}	β_c mV dec^{-1}	C.R. mpy	Θ	% IE
Blank	0	22	571	110	201	172.9	-----	-----
1	1	41	370	58	212	45.0	0.352	35.2
	5	11	282	68	158	44.8	0.506	50.6
	9	17	281	70	166	37.7	0.508	50.8
	13	14	224	70	185	14.3	0.608	60.8
	17	14	134	96	167	16.0	0.765	76.5
	21	6	127	65	195	17.2	0.777	77.7
2	1	11	412	85.3	150	55.2	0..278	27.8
	5	12	398	87	134	53.0	.303	30.3
	9	14	330	86	154	50.8	0..422	42.2
	13	40	254	73	193	40.5	0.555	55.5
	17	14	224	70	185	34.7	0.720	72.0
	21	35	130	70	203	23.1	0.772	77.2

Table 8. EIS procedure estimated electrochemical kinetic parameters in 1 M HNO_3 in absence and presence of different concentrations of compounds (1 and 2) at 25°C

Concentration, M		R_p, kΩ cm^2	C_{dl}, µF cm^{-2}	θ	% IE
1 M HNO3		28.9	1.4	---	---
1	1x 10^{-6}	169.0	5.6	0.829	82.9
	5x 10^{-6}	185.4	5.4	0.844	84.4
	9x 10^{-6}	385.7	5.3	0.925	92.5
	13x 10^{-6}	406.0	5.1	0.929	92.9
	17×10^{-6}	527.3	4.7	0.945	94.5
	21x 10^{-6}	534.3	4.7	0.956	95.6
2	1x 10^{-6}	143.5	5.6	0.799	79.9
	5x 10^{-6}	164.0	5.4	0.825	82.5
	9x 10^{-6}	178.0	5.3	0.839	83.9
	13×10^{-6}	195.0	5.1	0.853	85.3
	17x 10^{-6}	513.0	4.7	0.934	93.4
	21x 10^{-6}	537.0	4.7	0.936	93.6

Table 9. Electrochemical kinetic parameters acquired from EFM method for copper in 1M HNO_3 in the absence and presence of different concentrations of compounds

Comp.	Conc. M	$i_{corr,}$ µA cm^{-2}	β_a mVdec^{-1}	β_c mV dec^{-1}	CF-2	CF-3	C. R mpy	%IE
blank	1	391	60	174	1.913	2.939	197.5	-------
1	$1X10^{-6}$	106	57	99	1.918	3.362	53.5	72.9
	$5X10^{-6}$	89	55	122	1.961	2.471	44.9	77.3
	$9X10^{-6}$	64	65	194	1.974	2.792	32.2	83.7
	$13X10^{-6}$	57	59	104	1.872	2.583	28.2	85.4
	$17X10^{-6}$	22	75	183	1.761	2.323	11.3	94.3
	$21X10^{-6}$	21	53	117	1.858	3.790	10.7	94.6
2	$1X10^{-6}$	125	57	200	1.913	2.743	63.4	67.9
	$5X10^{-6}$	99	54	102	1.856	3.234	50.3	74.5
	$9X10^{-6}$	65	52	92	1.929	3.170	32.7	83.4
	13×10^{-6}	59	58	224	1.980	3.002	29.8	84.9
	$17X10^{-6}$	44	60	187	1.936	2.742	22.2	88.8
	$21X10^{-6}$	43	59	188	1.975	3.200	22.0	88.9

Table 10. Surface creation (weight %) of copper after 45 h of drenching in 1 M HNO_3+$21x10^{-6}$M of investigated inhibitors

Mass %	Cu	O	C
1	65.80	18.51	15.69
2	65.90	24.12	9.99

Table 11. E_{HOMO}, E_{LUMO}, kinetic gap (ΔE) and molecular area for the different compounds as obtained (PM3) method in gas phase.

parameters	2	1
$-E_{HOMO}$, eV	9.563	8.728
$-E_{LUMO}$, eV	1.208	1.023
ΔE, eV	8.355	7.700
Molecular Area	382.014	394.346
Dipole moment	7.642	12.441

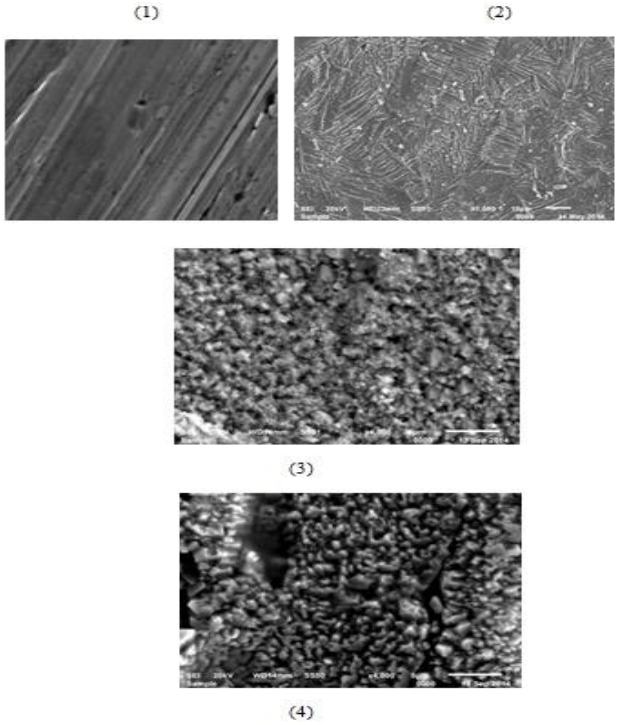

Figure 10. SEM micrographs of copper surface (1) before of immersion in 1 M HNO_3 (2) after 45 h of immersion in 1 M HNO_3, (3) after 45 h of immersion in 1 M HNO_3+ $21x10^{-6}$ M of compound 1,(4) after 45 h of immersion in 1 M HNO_3+ $21x10^{-6}$ M of compound 2 at 25°C

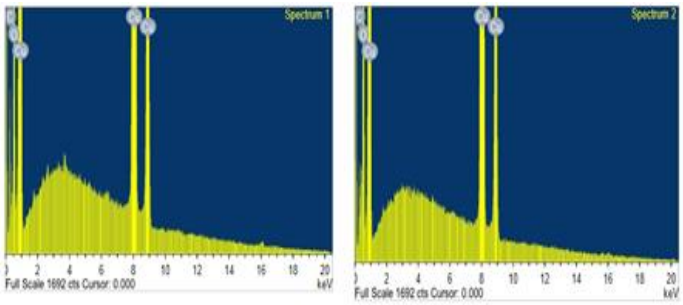

Figure 11. EDX spectra of copper in 1 M HNO_3 in the vicinity $21x\ 10^{-6}$M compound (1) and in $21x10^{-6}$ M compound (2) (b)

The HOMO–LUMO kinetic gap, ΔE approach, which is an imperative constant index, is connected to create theoretical models for clarifying the structure and adaptation hindrances in many molecular systems. The littler the estimation of ΔE, the more is the plausible inhibition productivity which the compound has [50-51]. It was demonstrated from (Table 11) that compound (1) has the littlest HOMO–LUMO hole compared with the other molecules. Accordingly, it could be expected that compound (1) molecule has more inclination to adsorb on the metal surface than the other molecules.

Variation in the inhibition efficiency of the inhibitors depends on the presence of electronegative O-, S- and N- atoms as substituent in their molecular structure. The calculated charges of selected atoms are presented in Fig. 12.

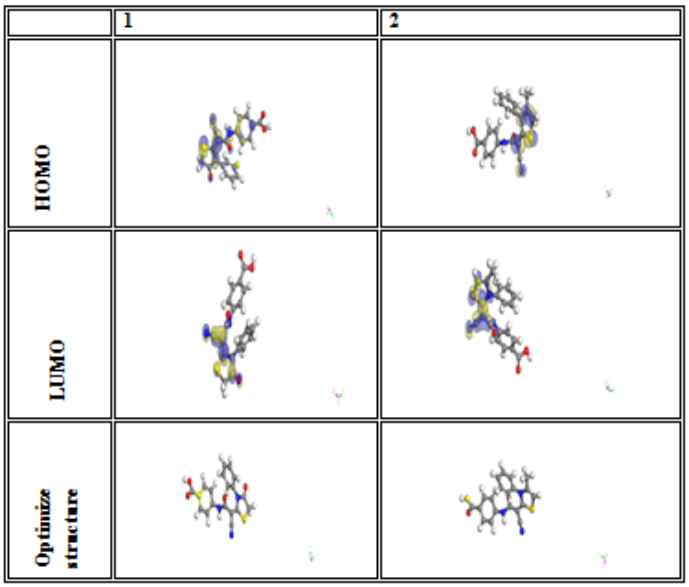

Figure 12. Optimized molecular structure of inhibitors (1, 2) and their frontier molecular orbital density distribution (HOMO and LUMO)

Instrument of corrosion inhibition

The inhibition instrument involves the adsorption of the inhibitor on the metal surface immersed in aqueous HNO_3 solution. Four types of adsorption[52] may take place involving organic molecules at the metal–solution interface: 1)Electrostatic attraction between the charged molecules and the charged metal; 2) Interaction of unshared electron pairs in the molecule with the metal; 3) Interaction of π-electrons with the metal; 4) Combination of all the above. From the observations drawn from the different methods, corrosion inhibition of copper in 1M HNO_3 solutions by the investigated inhibitors as indicated from weight loss, potentiodynamic polarization and EIS techniques were found to depend on the concentration and the nature of the inhibitor. The order of inhibition efficiency is as follows: 1>2

It has been beforehand reported in literature, that inhibiting impact depends for the most part on inhibitor concentration, the molecular structure, size and structure of the side chain in the organic compounds. Compound (1) contains 4O, 3N and one S atoms but compound (2) contains 3O, 3N and one S atoms. The highest inhibition efficiency was observed for compound (1) as it has an additional oxygen atom with lone pair of electrons. These electrons interact with the vacant d-orbital of copper and adsorb strongly thereby blocking more number of adsorption sites on the copper surface. In addition to compound (1) has higher molecular size than compound (2).

Conclusions

From the general test results the accompanying conclusions can be found:

1. The researched mixes are great inhibitors and go about as blended sort inhibitors for the corrosion of copper in 1 M HNO_3 solution.
2. Sensibly great assertion was seen between the qualities acquired by the WL and electrochemical estimations. The order of % IE of these researched mixes is in the following order: (1) > (2)
3. From all electrochemical estimations the outcomes which got from all electrochemical estimations demonstrated that the activity of any inhibitor increments with the expansion in inhibitor concentration and reductions with the raising the temperature.
4. Twofold layer capacitances diminish as for blank solution when the inhibitor is added. This truth affirms the adsorption of these molecules on the copper surface.
5. The adsorption of inhibitor on copper surface in HNO_3 solution follows Langmuir adsorption isotherm.
6. The negative qualities of ΔG°_{ads} show unconstrained adsorption of the inhibitors on the surface of copper Surface.
7. Quantum chemical parameters for these researched mixes were computed to give further understanding into the system of inhibition of the corrosion procedure.

References

1. Huilong, W., Jiashen Z., and Jing, L., *Anti-Corros. Methods and Mater.* 2002, 49, 127
2. Said, M. T., Ali, S. A., and Rahman, S.U., *Anti-Corros. Methods and Materials* 2003, 50, 201
3. Atia, A., and Saleh, M. M., *J. Appl. Electrochem.* 2003, 33, 171.
4. Tamilselvi, S. and Rajeswari, S., Anti-*Corros. Methods and Materials*, 2003, 50, 223.
5. Keera, S. T., *Anti-Corros. Methods and Materials*, 2003, 50, 280.
6. Chetouani A., Hammouti B.,.Aouniti A, Benchat N., Benhadda T., *Prog.Org.Coat.*, 2002, 45 373.
7.Bekkouch K., Aouniti A., Hammouti B., Kertit S., *J.Chim.Phys.*, 1999, 96, 838.
8. Kertit S., Hammouti B., Taleb M., Brighli M., *Bll.Electrochem*, 1997, 13, 241.
9.Bouklah M., Benchat N., Aouniti A., Hammouti B., Benkaddaddour M., Lagrenee M. Vezine H., Bentiss F., *Prog.Org.Coat.*, 2004, 51, 118.
10. Bentiss, F., Lagrenée, M., Traisnel, M. and Hornez, J. C., *Corros. Sci.*, 1999, 41, 789
11. Bentiss, F., Lagrenée, M. and Traisnel, M., *Corrosion.* 2000, 56, 733.
12. Bentiss, F., Traisnel, M. and Lagrenée, M., *J. Appl. Electrochem*., 2001, 31, 41.
13. Antonijevic, M.M.; Petrovic, M. B. *Int. J. Electrochem. Sci.* 2012, 7, 1.
14. Trachli, B.; Keddam, M.; Takenouti, H.; Srhiri, A. *Corr. Sci.* 2002, 44, 997.
15. Deslouis, C.; Tribollet, B.; Mengoli, G.M.; Musiani, M. *J. Appl. Electrochem*. 1988, 18, 374.
16. Rodrigues, P.R.P.; Aoki, I.V.; De Andrade, A.H.P.; De Oliveira, E.; Agostinho, S.M.L. *Brit.Corr. J.* 1996, 31, 305.
17. Frignani, A.; Tommesani, L.; Brunoro, G.; Monticelli, C.; Fogagnolo, M. *Corr. Sci.* 1999, 41, 1205.
18. Rodrigues, P.R.P.; Zerbino, J.O.; Agostinho, S.M.L. *Mat. Sci. Forum* 1998, 289, 1299.
19. Mountassir, Z.; Srhiri, A. *Corr. Sci.* 2007, 49, 1350
20. Growcock, F. B. and Lopp, V. R., *Corros. Sci.*, 1988, 28,397
21. Mu G.N. Zhao T.P., Liu M, Gu T., *Corrosion*, 1996, 52,853.
22. E. E. Oguzie: Mater. Letters, 59 (2005) 1076.
23. Khaled K. F., *Mater. Chem. Phys.*, 2008, 112, 290
24. Khaled K. F., J. Appl. Electrochem., 2009, 39, 429
25. Bosch R. W., Hubrecht J., Bogaerts W. F., Syrett B. C., *Corrosion* 2001, 57, 60.
26. Abdel–Rehim S. S., Khaled K. F., Abd–Elshafi N. S., *Electrochim. Acta*, 2006, 51, 3269
27. Geerlings, P., De Proft, F., and Langenaeker, W., *Chem. Rev.*, 2003,103, 1793.

28. Sastri, V. S. and Perumareddi, J. R., "Molecular Orbital Theoretical Studies of Some Organic Corrosion Inhibitors", *Corrosion*, 1997, 53, 617
29. Lukovits, I., Kalman, E. and Zucchi, F. *Corrosion*, 2001, 57, 3
30. Martınez, S., *Mater. Chem. Phys.*, 2003, 77, 97
31. Bentiss, F., Jama, C., Mernari, B., ElAttari, H., ElKadi, L., Lebrini, M., Traisnel, M., Lagrenee, M., *Corros.Sci.* 2009, 51, 1628.
32. Benabdellah, M., aouniti, A., Dafali, A., Hammouti, B., Benkaddour, M., Yahyi, A., Ettouhami, A., *Appl. Surf. Sci.*, 2006, 252, 8341.
33. Aksut, A. A., Lorenz, W. J. L. and Mansfeld, F., *Corros.Sci.* 1982, 22, 611
34. Lorenz, W. J. and Mansfeld, F, *Corros. Sci.*, 1981, 21, 647
35. Yurt A, Bereket G, Kivrak A, Balaban A & Erk B, *J Appl Electrochem*, 2005, 35, 1025.
36. Bentiss F, Traisnel M & Lagrenee M, *Corros Sci.*, 2000, 42, 127.
37. Durnie W, Marco R D, Jefferson A & Kinsella B, *J Electrochem Soc*, 1999, 146, 1751.
38. Banerjee G & Malhotra S N, *Corrosion*, 1992, 48, 10.
39. Hour T P & Holliday R D, *J Appl Chem*, 1953, 3, 502.
40 Riggs L O (Jr) & Hurd T J, *Corrosion*, 1967, 23, 252.
41. Schmid G M & Huang H J, *Corros Sci*, 1980, 20, 1041.
42. Bentiss F, Lebrini M & Lagrenee M, *Corros Sci*, 2005, 47, 2915.
43. Marsh J, Advanced Organic Chemistry, 3rd edn (Wieley Eastern, New Delhi), 1988.
44. Silverman D.C. and Carrico J. E., *Corrosion*, 1988, 44, 280.
45. Lorenz W. J.and Mansfeld F., *Corros.Sci.* 1981, 21, 647.
46. Macdonald D. D., Mckubre M. C., "Impedance measurements in Electrochemical systems," Modern Aspects of Electrochemistry, J.O'M. Bockris, B.E. Conway, R.E.White, Eds., Plenum Press, New York, 1982, 14, 61.
47. Mansfeld F.; *Corrosion*, 1981, 36, 301.
48. Gabrielli C., "Identification of Electrochemical processes by Frequency Response Analysis,"Solarton Instrumentation Group, 1980.
49. El Achouri M., Kertit S., Gouttaya H.M., Nciri B., Bensouda Y., Perez L., Infante M.R., Elkacemi K., *Prog. Org. Coat.*, 2001, 43, 267.
50. Macdonald J.R., Johanson W.B., in: J.R. Macdonald (Ed.), Theory in Impedance Spectroscopy, John Wiley& Sons, New York, 1987.
51. Mertens S. F., Xhoffer C., Decooman B. C., E. Temmerman, *Corrosion*, 1997, 53, 381.
52. Trabanelli G., Montecelli C., Grassi V., Frignani A., *J. Cem. Concur. Res.*, 2005, 35, 1804.
[46] Trowsdate A. J., Noble B., Haris S .J., Gibbins I.S. R., Thomson G. E., Wood G. C.,Corros. Sci., 38 (1996) 177.
[47] Reis F. M., De Melo H.G. and Costa I., Electrochim. Acta, 51 (2006) 17.
[48] Lagrenee M., Mernari B., Bouanis M., Traisnel M.& Bentiss F., Corros. Sci., 44 (2002) 573.
[49] Mc Cafferty E., Hackerman N., J. Electrochem. Soc., 119 (1972) 146.
[50] Ma H., Chen S., Niu L., Zhao S., Li S., Li D., J. Appl. Electrochem., 32 (2002) 65.
[51] Kus E., Mansfeld F., Corros. Sci. 48 (2006) 965.
[52] Caigman G. A., Metcalf S. K., Holt E. M., J.Chem. Cryst., 30 (2000) 415.
[53] Gao, G. and Liang, C. "Electrochemical and DFT studies of β-amino-alcohols as corrosion inhibitors for brass", Electrochim. Acta, 52(2007) 4554- 4559.
[54] Feng, Y., Chen, S., Guo, Q., Zhang, Y., Liu, G., *J. Electroanal. Chem*. 602 (2007) 115.
[55] Gece, G., Bilgic, S., *Corros. Sci*. 51 (2009) 1876.
[56] Martınez, S., *Mater. Chem. Phys*. 77 (2002) 97.
[57] Bereket, G., Ogretic, C., Ozsahim, C., *J. Mol. Struct. (THEOCHEM)* 663 (2003) 39.
[58] Li, W., He, Q., Pei, C., Hou, B., *Electrochim. Acta* 52 (2007) 6386.
[59] Rajenran, S., *J. Electrochem. Soc.* 54, (2005) 61
[60] Schweinsberg D. P., Graeme A., George, Nanayakkara A.K. and Steinert D.A., Corros. Sci., 28 (1988)